

Application of FT-IR Classification Method in Silica-Plant Extracts Composites Quality Testing

A Bicu¹, V Drumea¹, D E Mihaiescu^{2,*}, B Purcareanu¹, M A Florea¹, B Trică³,
G Vasilievici³, S Draga¹, E Buse¹ and L Olariu^{1,4}

¹S.C. BIOTEHNOS S.A., Gorunului Street No. 3-5, 075100 Otopeni, Ilfov, Romania

²Department of Organic Chemistry "Costin Nenitescu" Faculty of Applied Chemistry and Materials Science, Politehnica University of Bucharest, Polizu Street No. 1-7, 011061 Bucharest, Romania

³INCDCP-ICECHIM, 202 Spl. Independentei, 060021, Bucuresti, Romania

⁴ Academia Oamenilor de Stiinta din Romania, 54 Spl. Independentei, 050094, Bucharest, Romania

E-mail: danedmih@gmail.com

Abstract. Our present work is concerned with the validation and quality testing efforts of mesoporous silica - plant extracts composites, in order to sustain the standardization process of plant-based pharmaceutical products. The synthesis of the silica support were performed by using a TEOS based synthetic route and CTAB as a template, at room temperature and normal pressure. The silica support was analyzed by advanced characterization methods (SEM, TEM, BET, DLS and FT-IR), and loaded with *Calendula officinalis* and *Salvia officinalis* standardized extracts. Further desorption studies were performed in order to prove the sustained release properties of the final materials. Intermediate and final product identification was performed by a FT-IR classification method, using the MID-range of the IR spectra, and statistical representative samples from repetitive synthetic stages. The obtained results recommend this analytical method as a fast and cost effective alternative to the classic identification methods.

1. Introduction

Mesoporous materials have attracted great interest in current years because of the unusual mechanical, electrical and optical properties as a consequence of bulk and surface properties on the overall behaviour [1, 2, 9].

This type of materials are widely used in the industry for many applications, including adsorption, gas separation, catalysis, biological and medical fields [13-16].

In 2001, the first reported mesoporous silica material as a drug delivery system was MCM-41 (mobile composition of matter no.41). Type MCM-41 mesoporous silica materials are used as excellent carriers for drug delivery [17-20], for both systemic delivery systems and implantable local-delivery devices, due to the large surface area (800-1100 m²/g), arrangement and the adjustable size of mesopores between 2-8 nm. [10-12] Also, drug diffusion kinetics can be controlled due to the functionalization of silanol groups [3-5, 22]. These types of loaded materials have applicability in the pharmaceutical industry due to the slow release of active principles, as demonstrated by previous desorption studies. [18-20] MCM-41 has a loading capacity of up to 30 weight percent [25].



Content from this work may be used under the terms of the [Creative Commons Attribution 3.0 licence](https://creativecommons.org/licenses/by/3.0/). Any further distribution of this work must maintain attribution to the author(s) and the title of the work, journal citation and DOI.

The instrumental characterization of this material was achieved using microscopic methods as Transmission electron microscopy (TEM) to determine pore structure, Scanning electron microscopy (SEM) to determine particle morphology, spectroscopic method like Dynamic light scattering (DLS) to determine hydrodynamic particle diameter, other analyses like Brunauer–Emmett–Teller (B.E.T.-specific surface area (SSA) to determine pore volume and diameter and X-ray diffraction (XRD) to determine crystalline structure and pore geometry [7].

Generally, pharmaceutical agents have a specific chemical structure and target a specific molecular receptor. Naturopathic medicine is less specific and uses naturally occurring materials, such as plant extracts and herbs. Based on its advantages – sensitivity, selectivity and speed, Fourier transform infrared (FT-IR) can serve as an optimal tool for the analysis of plant extracts [21].

In this paper, we used a FT-IR classification method (MID-range of the IR spectra) in order process validation and class identification. The techniques used in the pharmaceutical industry to facilitate the identification of raw materials and intermediates for obtaining the finished product.

2. Materials and methods

2.1. Materials

For MCM-41 synthesis we used the following high purity reagents:

- Tetraethyl orthosilicate (TEOS, Sigma- Aldrich);
- Hexadecyltrimethylammonium bromide (CTAB, > 99% purity, Sigma- Aldrich);
- Sodium hydroxide (> 98% purity, Sigma- Aldrich);
- Acetic acid (100% purity, Sigma- Aldrich);
- Commercial MCM-41 purchase from Glantreo (MCM-41).

The loading process of the MCM-41 materials was performed using 2 natural hydroethanolic extracts (70% ethanol) of *Calendula officinalis* and *Salvia officinalis* [8]. The loading percentage was 28% (w/w).

2.2. Methods

2.2.1. MCM- 41 Synthesis. The mesoporous material was synthesized at room temperature by the sol-gel method using CTAB (hexadecyltrimethylammonium bromide) template and TEOS (tetraethyl orthosilicate) silicon source; the dried product was calcinated at 550⁰C for 24 h to remove the surfactant template and the calcined product was termed as MCM-41. [23] Loading was performed gradually, by solvent evaporation using a rotary evaporator under vacuum in order to maximize pore adsorption. For comparing the quality of MCM-41 obtained, we purchased commercial MCM-41 with the following specification: surface area 1098 m²/g, pore volume 0.8 cm³/g, pore diameter 4 nm and hexagonal pore geometry. This MCM-41 was loaded using the same method.

2.2.2 Characterisation MCM-41. SEM. Surface morphology was observed using the QUANTA INSPECT F electronic scanning microscope (SEM) equipped with EDX solid angle 0.13 (beam) with electron emission tunnel at 1.2 nm resolution.

HRTEM. High resolution images were collected by TecnaiTM G² F30 S-TWIN transmission electron microscope (FEI, the Netherlands) equipped with STEM/HAADF detector, EDX (Energy dispersive X-ray Analysis) and with an electron energy loss spectrometer EFTEM- EELS. The microscope operates at an acceleration voltage of 300 kV (Schottky field emitter) with a TEM point resolution of 2 Å and a TEM line resolution of 1.02 Å. The microscope was operated at an extracted voltage of 4500V.

DLS. Hydrodynamic particle radius measurements were carried out by using Malvern Nano ZS Zetasizer instrument. The measurement of size was performed with 0.3% suspensions of MCM-41 in ultrapurified water Milli-Q, at 25⁰C, after 10 min sonication, at an angle of 173°. For size determination, 5 measurements on each sample were carried out and the mean value was reported.

B.E.T. Nitrogen adsorption isotherms was measured at –196⁰C using Micromeritics apparatus ASAP 2420 (USA 2012). Prior to the experiment the sample was outgassed at 200⁰C in a vacuum for 1h. Gas-volumetric analysis, specific surface area (SSA), pore volume and size were measured by N₂

adsorption-desorption isotherms. SSA was calculated using the Brunauer-Emmett-Teller (BET) method.

UV-VIS. The desorption studies were performed using an on-flow system- Thermo Scientific Evolution 220 UV-VIS Spectrophotometer and peristaltic pump. The desorption curves were carried out in a 60 % ethanol/ 40 % ultrapurified water (Milli-Q system), at a spectral wavelength $\lambda = 205$ nm, at 5 minutes intervals for 20 hours.

FT-IR. The MIR spectra of samples were recorded from 4000 to 600 cm^{-1} with a HATR-FTIR diamond crystal infrared spectrometer (Spectrum BX II, Perkin-Elmer). Approximately 5–10 mg of sample were placed on the surface of the diamond crystal and measured directly. Intact MCM-41 and MCM41-loaded were analyzed by gently pressing the adaxial sample side in the region of the central lamina on to the HATR crystal. Background spectra was determined and subtracted from each sample spectrum; 32 acquisition per sample were performed, with a spectral resolution of 8 cm^{-1} . All sample acquisitions were performed in duplicate.

Each FT-IR spectrum can express a unique “fingerprint”, which allows FT-IR spectroscopy to be used for identification of unknown samples and classification of different samples [24].

3. Results and discussions

To show that our synthesized MCM-41 is similar to MCM-41, we compared the characteristics of both materials using the instrumental methods mentioned.

From the DLS analysis we concluded that the particle average size of our synthesized MCM-41 (2623 nm) is very close to particle average size of MCM-41 (2375 nm). The polydispersity index of synthesized MCM-41 (PDI=0.478) has a smaller value than the MCM-41 (PDI= 0.797); this shows that our mesoporous material has a better particle size distribution, therefore the material adsorption/desorption is conducted more efficiently.

Surface morphology analysis (SEM) reveals a heterogeneous structure (shape and size), with intergranular spaces and randomly distributed agglomerations (Figure 1). After magnification one can observe a porous ultrastructure in the 1 - 2 microns scale, given by the mesopore structure (better emphasized in the HRTEM analysis).

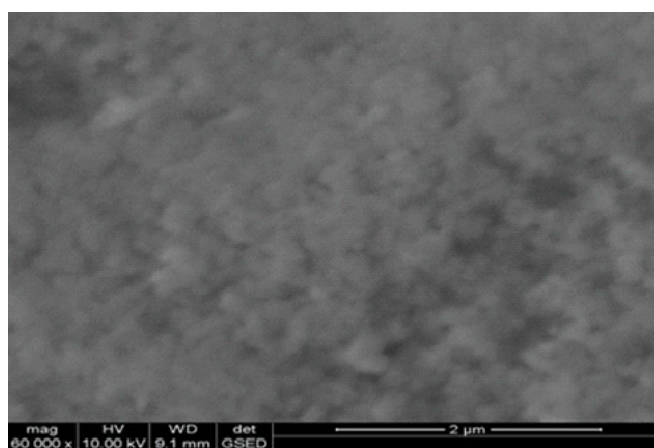


Figure 1. SEM morphology of the synthesized MCM-41.

In the image obtained by HRTEM (Figure 2) we can observe the hexagonal pore structure with medium ordering and mesoporous dimensions of 2-4nm, characteristics allowing the classification of the obtained material in the MCM-41 category. This structure allows efficient loading, due to the high pore diffusion rate of the loaded material as well as a higher diffusion accessibility in the desorption processes.

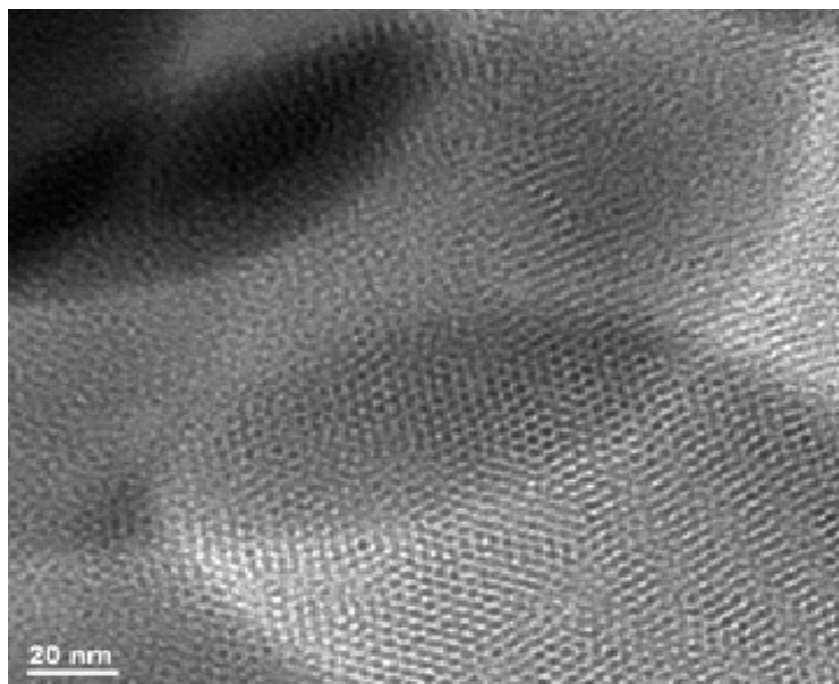


Figure 2. HRTEM of the synthesized MCM-41.

B.E.T. results for MCM-41-Synthesized- B.E.T. Surface Area: 1224.34 m²/g and BJH Adsorption average pore diameter (4V/A): 2.44 nm. The results show that this material can be classified as MCM-41.

From the FT-IR spectra (Figure 3), the specific bands for synthesized MCM-41 and MCM-41 are: 803 cm⁻¹, 1050 cm⁻¹, 1627 cm⁻¹ and 3375 cm⁻¹.

As proof of adsorption using *Calendula officinalis* hydroethanolic extract, the following FT- IR spectra specific bands of MCM-41-Calendula were identified: 977 cm⁻¹, 1409 cm⁻¹ and 2935 cm⁻¹. Similarly, the FT-IR spectra of MCM-41-Salvia shows specific bands for hydroethanolic extract of *Salvia officinalis*: 969 cm⁻¹, 1413 cm⁻¹, 1547 cm⁻¹, 1691 cm⁻¹ and 2930 cm⁻¹.

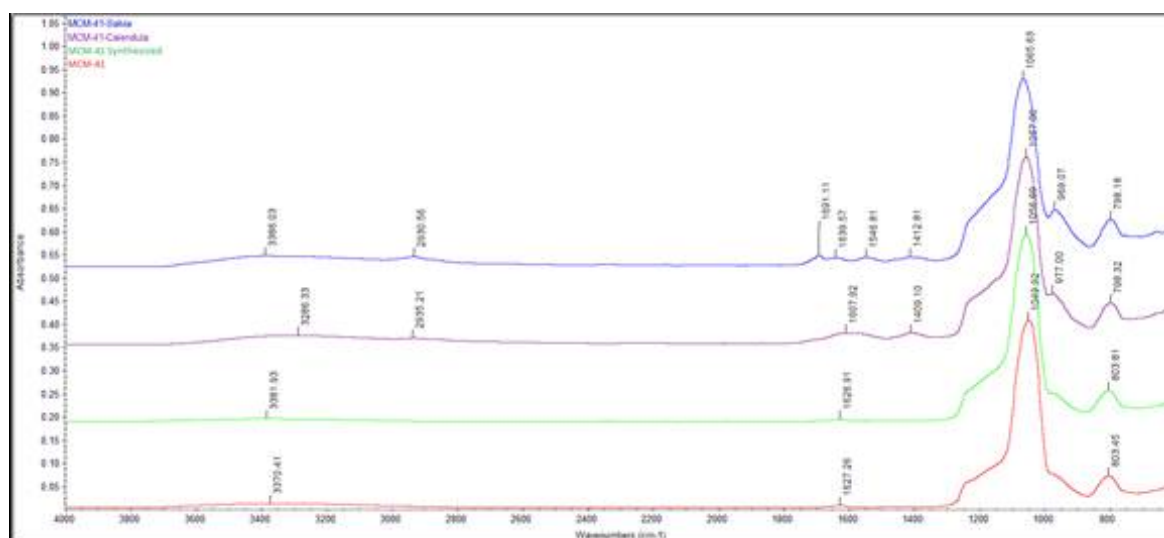


Figure 3. FT-IR spectra of MCM-41-Salvia, MCM-41-Calendula, MCM-41 Synthesized and MCM – 41.

3.1. Classification method by Discriminant analysis

Discriminant analysis was performed with the TQ Analyst 7.2.0 Thermo Electron software, using the following parameters: pathlength type: multiplicative signal correction (MSC), number of classes: 3 (salvia, calendula, MCM-41), 36 IR spectra, data format: first derivative, Savitzky-Golay filter, 23 data points, polynomial order 1 spectrum range: 1779.8 – 1287.7 cm^{-1} , baseline type: one point at 1800 cm^{-1} . For each class (class I: MCM-41 synthesized and MCM-41, class II: MCM-41-Calendula and class III: MCM-41-Salvia), FT-IR spectra for 6 different batches were determined in duplicate.

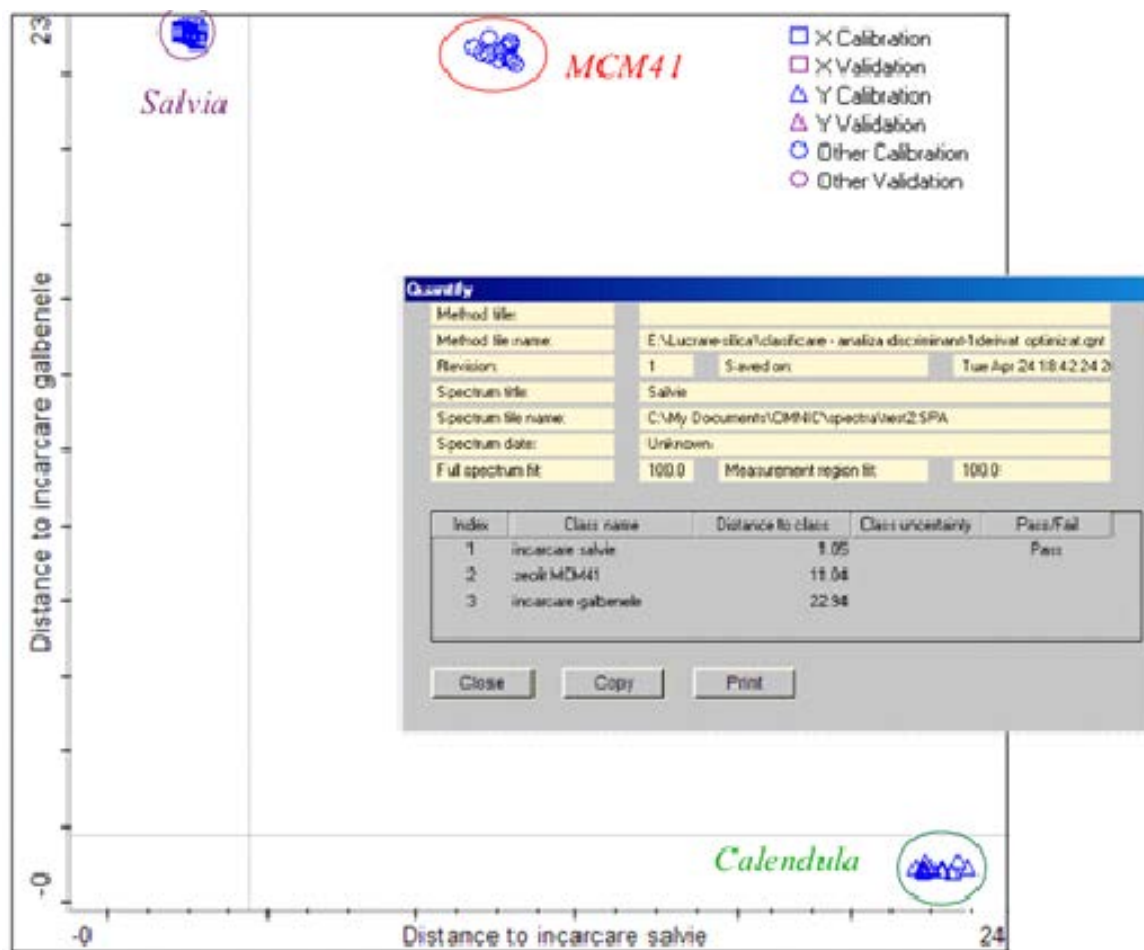


Figure 4. Calibration results for Salvia, Calendula and MCM-41 classes (by using 36 IR spectra), and quantification results for a Salvia validation sample.

Each sample was classified based on Mahalanobis distance. The developed method for sample classification is exemplified in Figure 4, where the Mahalanobis distance between classes is greater than 10, and the distance between members of the same class is less than 1.2.

To verify the selectivity of the method, another 18 samples from different batches (MCM-41, MCM-41-Calendula, MCM-41-Salvia) and 3 samples of MCM-41 loaded with other 3 plant extracts were analyzed (results shown in Table 1).

From the 21 samples, 6 of them passed the distance to class MCM-41 with a value between 0.78-0.99, 6 of them passed the distance to class MCM-41-Calendula with a value between 0.83-0.92, 6 of them passed the distance to class MCM-41-Salvia with a value between 0.91-1.13 and the other 3 samples did not match any of the classes.

Table 1. Results of sample tests.

No.	Sample Name	Distance to Class MCM-41	Distance to Class MCM-41-Calendula	Distance to Class MCM-41-Salvia	PASS/ FAIL
1	Test 1	22.45	0.83	22.91	PASS Calendula
2	Test 2	11.04	22.94	1.05	PASS Salvia
3	Test 3	0.99	22.68	10.72	PASS MCM-41
4	Test 4	22.45	0.83	22.91	PASS Calendula
5	Test 5	22.68	0.89	23.13	PASS Calendula
6	Test 6	22.7	0.81	23.26	PASS Calendula
7	Test 7	22.85	0.92	23.45	PASS Calendula
8	Test 8	22.57	0.87	23.12	PASS Calendula
9	Test 9	10.8	23.16	0.91	PASS Salvia
10	Test 10	11.32	23	1.02	PASS Salvia
11	Test 11	10.78	23.08	1.01	PASS Salvia
12	Test 12	11.02	22.82	1.1	PASS Salvia
13	Test 13	11.05	23.11	1.13	PASS Salvia
14	Test 14	0.99	22.68	10.72	PASS MCM-41
15	Test 15	0.96	22.96	10.92	PASS MCM-41
16	Test 16	0.78	22.37	11.16	PASS MCM-41
17	Test 17	0.9	22.55	10.8	PASS MCM-41
18	Test 18	0.87	22.82	11.18	PASS MCM-41
19	Test 19	81.09	80.35	80.61	FAIL
20	Test 20	31.73	19.35	29.33	FAIL
21	Test 21	22.01	9.17	29.85	FAIL

3.2. Desorption studies

The desorption study was performed with 60% ethanol/40% ultrapurified water Milli-Q system, at 35°C, under continuous stirring, undersolution recirculation. The determinations were performed, in both cases, at a wavelength $\lambda = 205$ nm. In the case of the desorption study for the materials loaded with Salvia extract, a similar profile is observed for both samples, concluding that the two materials show a slow release for 20 hours (Figure 5).

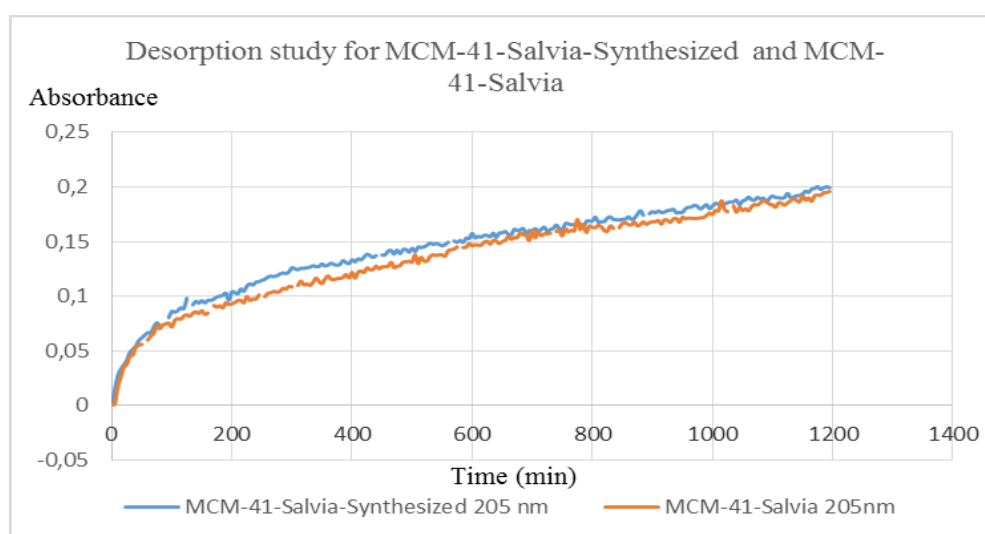


Figure 5. Desorption study for MCM-41-Salvia-Synthesized and MCM-41-Salvia.

In the case of the desorption study carried out on the two materials loaded with Calendula extract, showed the same slow release, with the observation that MCM-41-Calendula, after 7 hours, the slow release of the active principles stops, compared to MCM-41-Calendula-Synthesized where slow release continues for up to 20 hours (Figure 6).

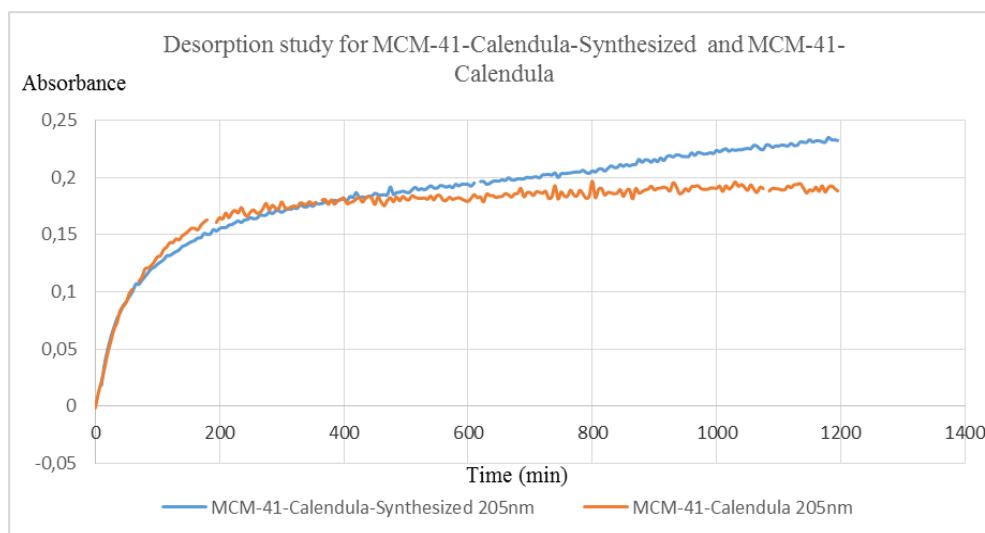


Figure 6. Desorption study for MCM-41-Calendula-Synthesized and MCM-41-Calendula.

4. Conclusions

We obtained a mesoporous material that is comparable, in regard to its characteristics, with the purchase mesoporous material. Both types of MCM-41 were loaded with different total plant extracts.

Desorption curves were used to evaluate the slow release profiles, which is a very valuable parameter for multiple applications in the pharmaceutical industry.

The required identification step for the product technical data sheet was performed using the FT-IR classification method, demonstrating the statistical homogeneity of the experimental data. The FT-IR classification method is a quick tool for sample classification, being able to discriminate between various loading materials.

5. References

- [1] Wu S H, Mou C Y and Lin H P 2013 *Chemical Society Reviews* **42** 3862-75
- [2] Rahman N A, Widhiana I, Juliastuti S R and Setyawan H 2015 *Colloids and Surfaces A: Physicochem. Eng. Aspects*, **476** 1-7
- [3] Mihaiescu D E, Tamas D, Andronescu E and Ficai, A 2014 *Digest Journal of Nanomaterials and Biostructures*, **9(1)** 379-83
- [4] Tameemi Al MBM, Mihaiescu D E, Stan R, Meghea A, Voicu G, Vasile B S, Traistaru V and Istrati D 2015 *Digest Journal of Nanomaterials and Biostructures* **10(4)** 1229-53
- [5] Al Tameemi MBM, Gudovan D, Stan R, Mihaiescu D E and Ott C 2015 *Romanian Journal of Materials* **45(2)** 188-193
- [6] Li T, Chen X, Liu Y, Fan L, Lin L, Xu Y, Chen S and Shao J 2017, *European Journal of Pharmaceutical Sciences* **96** 456-463
- [7] Fudulu A, Dumitriu B G, Olariu L, Buse E and Mihaiescu D E 2017 *The FEBS Journal* **284** (Suppl. 1) 335
- [8] Dumitriu B G, Olariu L, Ene M D and Rosoiu N 2013 *Romanian Biotechnological Letters* **18(3)** 8284-94

- [9] Vaghasiya J V 2017 *J Mater Sci Nanomater, Innovations in Engineered Mesoporous Material for Energy Conversion and Storage Applications* **1**(1)
- [10] Grumezescu A M, Mihaiescu D E and Tamas D 2011 *Biointerface Research in Applied Chemistry* **1**(6) 229-235
- [11] Mihaiescu D E, Tamas D, Andronescu E and Ficai A 2014 *Digest Journal of Nanomaterials and Biostructures* **9**(1) 379-383
- [12] Mihaiescu D E, Gudovan D and Marton A 2014 *Revue Roumaine de Chimie* **59**(2) 111-116
- [13] Sun M, Chen C, Chen L and Su B 2016 *Frontiers of Chemical Science and Engineering, Hierarchically porous materials* **3**(10) 301– 347
- [14] Anis S F, Khalil A, Saepurahman, Singaravel G, and Hashaikeh R 2016 *Microporous and Mesoporous Materials* **236** 176– 192
- [15] Parak W J, Gerion D, Pellegrino T et al. 2003 *Nanotechnology* **7**(14) R15–R27
- [16] Danilczuk M, Długopolska K, Ruman T and Pogocki D 2008 *Mini reviews in medicinal chemistry* **13**(8) 1407–17
- [17] Berlier G, Gastaldi L, Sapino L, Miletto I, Bottinelli E, Chirio D and Ugazio E 2013 *International Journal of Pharmaceutics* **457** 177–186
- [18] Ambrogi V, Latterini L, Marmottini F, Tiralti M C and Ricci M 2013 *J Pharm Innov* **8** 212–217 DOI: 10.1007/s12247-013-9161-2
- [19] Bodana P, Kelkar G, Manglavat S K, Gupta A K and Chaturvedi S C 2016 *Int.J.Adv.Res* **4**(12) 2518-30 DOI:10.21474/IJAR01/2677
- [20] Stefanache A, Ignat M, Peptu C A, Diaconu A, Stoleriu I and Ochiuz L 2017 *Appl. Sci.* **7** 237 DOI: 10.3390/app7030237
- [21] Thermo Fisher Scientific, *Application Note: 51254*
- [22] Mehmood A, Ghafar H, Yaqoob S, Gohar U F and Ahmad B 2017 *J Develop Drugs*, **6**(2) DOI: 10.4172/2329-6631.1000174
- [23] Istrati D et al. 2015 *Revue Roumaine de Chimie*, **60**
- [24] Cao Z, Wang Z, Shang Z and Zhao J 2017 *PLoS ONE* **12**(2) e0172359, DOI:10.1371/journal.pone.0172359
- [25] Sang W Y and Ching O P 2017 *Tailoring MCM-41 Mesoporous Silica Particles through Modified Sol-Gel Process for Gas Separation* DOI: 10.1063/1.5005480

Acknowledgement

This study was financed by the Romanian Research Authority, contract 49 PTE/2016.